

A Kinetic Model of UO_2 Dissolution in Acid, H_2O_2 Solutions That Includes Uranium Peroxide Hydrate Precipitation

L. E. EARY and L. M. CATHLES

Laboratory experiments have been carried out to determine the dissolution kinetics of UO_2 in the $\text{UO}_2\text{-H}_2\text{O}_2\text{-SO}_4\text{-H}_2\text{O}$ system under conditions similar to those which occur during acid *in situ* leaching of sandstone uranium deposits. UO_2 dissolution proceeds by an electrochemical reaction at the UO_2 surface. Sulfate ions adsorb onto the UO_2 surface and reduce the rate of UO_2 dissolution by blocking sites of potential oxidation. UO_2^{2+} precipitates as insoluble uranium peroxide hydrate ($\text{UO}_4 \cdot \text{XH}_2\text{O}$), and under even moderate pH conditions can greatly reduce the UO_2 dissolution rate. The overall UO_2 dissolution (including $\text{UO}_4 \cdot \text{XH}_2\text{O}$ precipitation) can be usefully described by a simple kinetic model that considers dissolution and precipitation to be independent processes. The model has the advantage that the dissolution rate at a given temperature is a function only of solution composition and UO_2 surface area. The chemical model can thus be easily combined with fluid flow models to obtain a full chemical-physical model of the leaching of uranium ore in a column experiment or *in situ*.

I. INTRODUCTION

SANDSTONE uranium deposits constitute the largest source of low-cost uranium reserves in the United States. The richest and most accessible deposits have been, or are, being mined by conventional open pit or underground methods. However, direct recovery of uranium from low grade sandstone deposits by *in situ* leaching is a viable alternative to conventional methods of uranium mining that is presently being used to recover uranium from roll front deposits in Wyoming and south Texas.

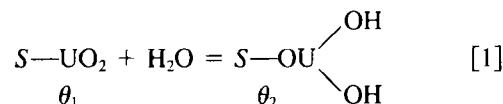
Knowledge of the chemistry and kinetics of UO_2 dissolution is necessary if *in situ* leaching processes are to be understood and optimized, and could provide a basis for design and optimization of acid vat leaching of uraninite concentrate. This paper reports the results of initial rate experiments designed to determine the dissolution rate of UO_2 in acid solutions containing H_2O_2 and conditions similar to those expected in an acid *in situ* leach operation (Table I). An expression is derived that gives the rate of UO_2 leaching as a function of H_2O_2 and total sulfate concentrations and pH. The mechanism of UO_2 dissolution is described. UO_2 dissolution by H_2O_2 is a particularly interesting process because, even at low pH conditions, a uranium peroxide hydrate ($\text{UO}_4 \cdot \text{XH}_2\text{O}$) forms on the uraninite grains, and this precipitation affects the dissolution kinetics. The mathematical model derived from the experiments takes into account the effects of uranium peroxide hydrate precipitation on UO_2 dissolution kinetics, and is consistent with the experiments and theories of heterogeneous reaction kinetics.

The mechanisms of reactions in heterogeneous systems, including the UO_2 dissolution reaction considered in this paper, often involve a similar series of steps:

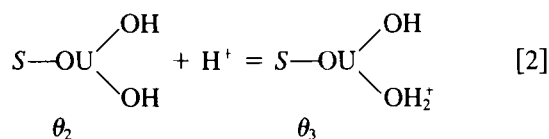
- “(1) adsorption of fluid species onto surface,
- (2) reaction of adsorbed species among themselves or with the surface atoms, and

- (3) desorption of product species.” (Lasaga²)

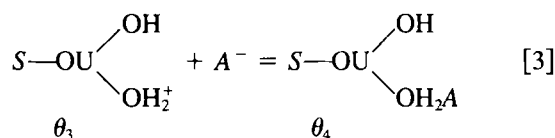
Interactions at the oxide-water interface have been described in general by Parks³ and Davis.⁴ First a hydroxylated surface can be expected to form on any metal oxide in an aqueous environment and can be represented as shown in reaction [1] for the UO_2 surface. The symbols θ_1 - θ_3 represent the fraction of the oxide surface present as the indicated surface species. S indicates the surface.



The hydroxylated surface may develop a charge due to amphoteric protonation or dissociation of the adsorbed hydroxyl groups. Protonation, reaction [2], is much more likely at the low pH values used in the dissolution experiments (Table I). The zero point of charge for UO_2 has been shown to occur at pH values of 4.5 to 6.0 (Maroto⁵ and Parks⁶).



Furthermore, anions, A^- , present in solution adsorb onto the oxide surface. Anions may adsorb either to charged sites as indicated by reaction [3], or possibly, to θ_1 sites.



Adsorption of anions which do not contribute to the oxidation of UO_2 , or do not desorb easily, will slow the oxidation reaction by competing with reactants for active oxidation sites.

In this paper it is proposed that UO_2 dissolution proceeds by the following series of steps. First, H_2O_2 molecules are adsorbed onto the UO_2 surface forming a surface peroxide complex. H_2O_2 may adsorb directly at θ_1 sites as shown by

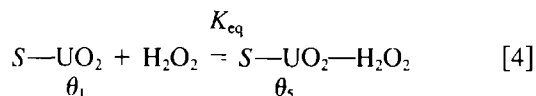
L. E. EARY is Graduate Student, Department of Geosciences, Pennsylvania State University, University Park, PA 16802. L. M. CATHLES, formerly Associate Professor of Geosciences, Department of Geosciences, Pennsylvania State University, University Park, PA, is now Senior Research Geophysicist with Chevron Oil Field Research Company, La Habra, CA 90631.

Manuscript submitted March 19, 1982.

Table I. Comparison of the Chemical Conditions of Our Experiments to Those of an Acid *in situ* Leach Operation (from Tweeton¹). The Compositional Ranges Reported by Tweeton,¹ *et al* (1978) Reflect a 140-Day Period of Solution Injection and Recovery.

	Acid <i>in situ</i> Leach Conditions	Experiments in This Study
temperature	11 to 16 °C	25 to 50 °C
pressure	up to 15 bars	1 bar
H ₂ O ₂ injection concentration	2 × 10 ⁻⁶ to 3 × 10 ⁻⁴ M	1 × 10 ⁻⁶ to 1 × 10 ⁻² M
pH	5.5 to 1.4	4.8 to 1.2
SO ₄ ²⁻	2000 to 7700 ppm	0 to 6000 ppm
UO ₂ ²⁺	30 to 300 ppm	1 ppb to 60 ppm

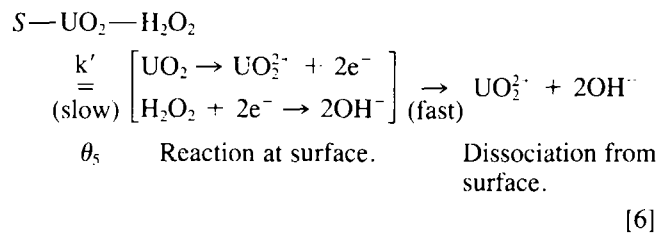
reaction [4] or at other sites θ_2 , θ_3 , or θ_4 after displacement of the other adsorbed species.



By analogy with other adsorption reactions it is expected that reaction [4] will take place quickly and reversibly in equilibrium with the surrounding solution (Lasaga²). The concentration of surface peroxide complexes is given by:

$$\theta_5 = \theta_1 K_{\text{eq}} [\text{H}_2\text{O}_2] \quad [5]$$

Oxidation of UO₂ occurs at surface peroxide complexes by an electrochemical mechanism. The mechanism involves the simultaneous anodic oxidation of UO₂ and cathodic reduction of H₂O₂ at surface complexes on the UO₂-surface interface. Nicol and Needes^{7,8} have established that the dissolution of UO₂ in the presence of chemical oxidants involves an electrochemical mechanism. The reaction at the surface is:



The surface reaction involves the transfer of two electrons from UO₂ to H₂O₂ in the surface peroxide complex. This electron transfer step is the slow step of the overall reaction and has rate constant k' . The products of the oxidation-reduction step are expected to dissociate quickly from the surface as indicated by the second step of reaction [6]. Steady state is assumed for this desorption step. Since the surface reaction is expected to be the slowest step, then using Eq. [5] the rate of this slow step and of the overall reaction is given by Eq. [7]:

$$\text{rate} = k' \theta_1 K_{\text{eq}} [\text{H}_2\text{O}_2] \quad [7]$$

We expect the oxidation of uraninite to be described by an equation of the form of Eq. [7], provided uranium does not precipitate from solution. The formation of a uranium per-

oxide hydrate precipitant on UO₂ grains was reported by Amell and Langmuir⁹ in two dissolution experiments involving H₂O₂ solutions.

II. EXPERIMENTAL

Uranium dioxide for dissolution experiments was obtained in 15 gram sintered pellets from the Westinghouse Corporation, Cheswick, Pennsylvania. Initial X-ray analysis indicated the material was stoichiometric UO₂ with unit cell length, $a = 5.470 \text{ \AA}$ (Gronvold¹⁰).

Before dissolution experiments began, the UO₂ pellets were crushed to particle size of 0.25 to 1.19 mm in diameter. The UO₂ grains were recrystallized in a Barnes¹¹ type rocking autoclave for two days at 300 °C in 0.5 M NaHCO₃ solution with a methane atmosphere, and then cooled over seven days to 100 °C. This process minimized factors that could affect solubility such as surface energy and surface preoxidation. Surface areas of the recrystallized grains were measured in two 25 gram batches by the Micromeritics Materials Analysis Laboratory, Norcross, Georgia, using krypton gas adsorption and BET calculation. The specific surface areas of the two samples were: 75 cm²/g ± 0.45 pct and 58 cm²/g ± 0.40 pct.

The total surface area of UO₂ grains used in dissolution experiments ranged from 25 to 50 cm². For experiments with low H₂O₂ concentrations (10⁻⁶ to 10⁻⁵ M) larger surface areas of 40 to 50 cm² were used to increase the amount of uranium dissolved.

Dissolved uranium concentrations were determined by the fluorimetric method.¹² Hydrogen peroxide determinations were made by a colorimetric method.¹³ Hydrogen ion activity was measured with a combination pH-reference electrode and pH meter.

Experiments were done in the system shown in Figure 1. Uraninite grains were sandwiched between two porous screens and placed on a platform in 1000 ml glass kettles. Gas tight adapters for the sampling tube, thermocouple (or pH electrode), N₂ inlet-outlet, and a separatory funnel were fitted into the top cap of the reaction kettle. An atmosphere of N₂ gas was used in the kettle to provide a non-oxidizing medium above the leaching solutions. The kettles were immersed up to the top cap in a temperature bath.

A magnetic stirrer driven by a water line from a submersible water pump was mounted below the kettle to rotate a stir bar within the kettle. Stirring speed could be controlled by adjusting the flow rate in the water lines leading to the magnetic stirrers. Adjustment, however, was qualitative and could only be described as none, very slow, medium slow, medium, or fast. The stir bar induced circulation through a set of plexiglass fins attached tangentially about the UO₂ grain platform within the kettle.

The pH of run solutions was adjusted by adding concentrated HCl dropwise until the starting pH value was reached. At low uranyl concentration (1 ppb to 60 ppm) and low chloride concentrations (less than 0.06 M in our experiments) chloride complexing does not appreciably increase UO₂ solubility (Smith and Martell¹⁴).

Dissolution rates were determined in the following manner: Five milliliters of leaching solution were drawn from the reaction kettle to rinse the sampling tubes and discarded. Solution samples, 10 ml each, were then drawn out and analyzed. Plots were made of total mg of UO₂ dissolved vs

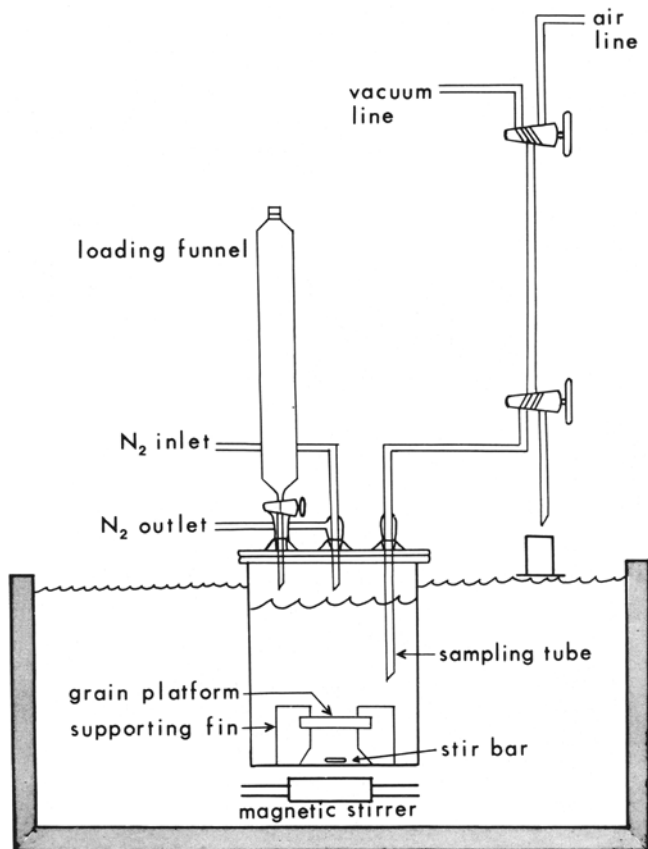


Fig. 1 — Experimental system.

time (hours). If a plot indicated a linear relationship, the dissolution rate was determined from the slope of the line. Slopes were determined by linear regressions of the plotted data. These slopes were then divided by the surface area, cm^2 , of the UO_2 grains reacted in that particular experiment, by the concentration of H_2O_2 in solution, g/cm^3 , and by the ratio of the molecular weight of UO_2 to the molecular weight of H_2O_2 (α) to obtain the mass transfer coefficient of the oxidation reaction, r . Note that the rate of dissolution of UO_2 in g/cm^2 per second is just the product of r , the concentration of H_2O_2 in solution in g/cm^3 , and the ratio of the molecular weight of UO_2 to the molecular weight of H_2O_2 . Plots of mg UO_2 dissolved vs time that were nonlinear because of uranium peroxide hydrate precipitation were treated in a different manner and are discussed in detail in a later section.

III. RESULTS

Before $\text{UO}_2 + \text{H}_2\text{O}_2$ dissolution experiments began it was determined that H_2O_2 decomposition in the reaction system was not important until temperatures of greater than 55°C were reached.

In the course of experimentation it was found that pH strongly affected UO_2 dissolution rate when raised above a certain value that depended on the H_2O_2 concentration of the leaching solution. This was due to the precipitation of uranium peroxide hydrate on the surface of the UO_2 grains. Below the critical pH value for any one H_2O_2 concentration, dissolution rate was independent of pH. Experiments

directed at determining the effect of stirring speed, temperature, H_2O_2 and sulfate concentration were conducted at pH and H_2O_2 concentrations in the region of pH independent dissolution. These experiments are discussed below in the section subtitled "pH Independent Dissolution." In a second section, "pH Dependent Dissolution," uranium peroxide hydrate precipitation is discussed.

A. pH Independent Dissolution

The dependence of the mass transfer coefficient on stirring rate was first measured. The effects of stirring a 1.0×10^{-2} M H_2O_2 , $\text{pH} = 1.5$ solution is shown in Figure 2. Figure 2 shows measurements of the mass transfer coefficient are independent of stirring speed for stirring speeds greater than "medium." This independence suggests that at stirring rates greater than medium the dissolution reaction at the UO_2 surface is the rate controlling process, not solution mass transfer. This suggestion is independently confirmed by two further observations: (1) Assuming an aqueous diffusion constant of 2×10^{-5} cm per second for H_2O_2 , an unreasonably large aqueous boundary layer of 1.0 cm thickness would be required to explain the 0.15×10^{-4} cm per second mass transfer coefficient of Figure 2. (2) The morphology (etch patterns) of leached UO_2 grains indicates surface rate control, not aqueous diffusion control. (Etch patterns are discussed below.) Subsequent dissolution experiments were conducted with a "fast" stirring speed.

Next, the dependence of the mass transfer coefficient on H_2O_2 concentration was determined by measuring initial dissolution rates for nine H_2O_2 concentrations at 25°C . H_2O_2 concentrations ranged from 10^{-6} to 10^{-2} M. All other variables were held constant. Four to eight runs, lasting 5 to 23.5 hours each, were completed at each of the nine H_2O_2 concentrations. For each H_2O_2 concentration the calculated

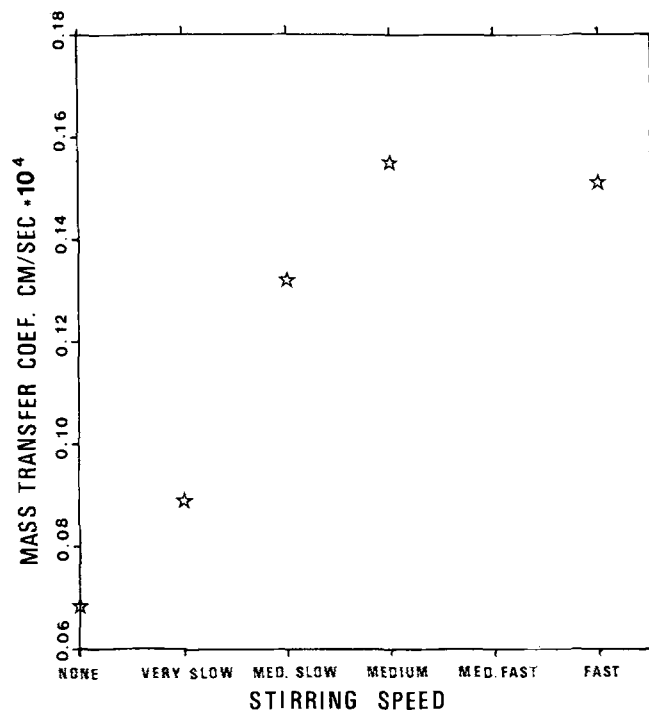


Fig. 2 — Mass transfer coefficient of H_2O_2 , r , as a function of stirring speed in the reaction kettle at 25°C . H_2O_2 concentration = 1×10^{-2} M.

dissolution rates were arithmetically averaged to give a mean rate for each concentration and a standard deviation about the mean. The data are plotted in Figure 3. The figure shows a linear dependence between the dissolution rate of UO_2 and H_2O_2 concentration (slope = 1.01 ± 0.10). Thus, the mass transfer coefficient is independent of H_2O_2 concentration. The best fit value of the mass transfer coefficient is:

$$r = (17.8 \pm 2.0) / [(3600) (MW_{\text{H}_2\text{O}_2}) (\alpha)]$$

that is:

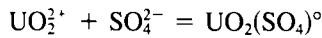
$$r = 1.8 \times 10^{-5} \text{ cm/sec} \quad [8]$$

where 3600 is the number of seconds in one hour.

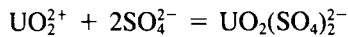
Figure 4 shows the mass transfer coefficient has an activation energy of 27.4 ± 2.3 kJ/mole (6.6 ± 0.6 kcal/mole) and that the activation energy is independent of H_2O_2 concentration for the temperature range, 25 to 50 °C.

These experiments establish that UO_2 dissolution rate can be described by a simple mass transfer coefficient. It should be noted, this is true only in cases where dissolution rates were found to be independent of pH. Increasing the pH of the leaching solution to conditions of uranium peroxide hydrate precipitation had the effect of decreasing the dissolution rate, as does the presence of sulfate in the leaching solution.

In acid *in situ* leaching sulfate is the most important complexing ligand for aqueous uranyl ion (Langmuir¹⁵ and Smith and Martell¹⁴). Two complexes are important:



and



The effect of total sulfate on UO_2 dissolution rate was measured for two H_2O_2 concentrations, 1×10^{-3} and 5×10^{-4} M, at five ratios of sulfate to bisulfate. Five

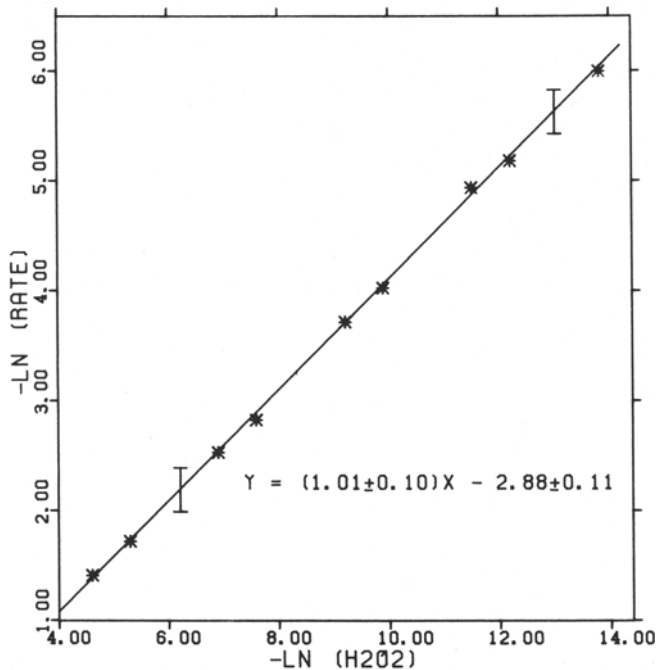


Fig. 3—Dissolution rate ($\text{mg UO}_2/\text{cm}^2/\text{h}$) as a function of H_2O_2 concentration (M) at 25 °C.

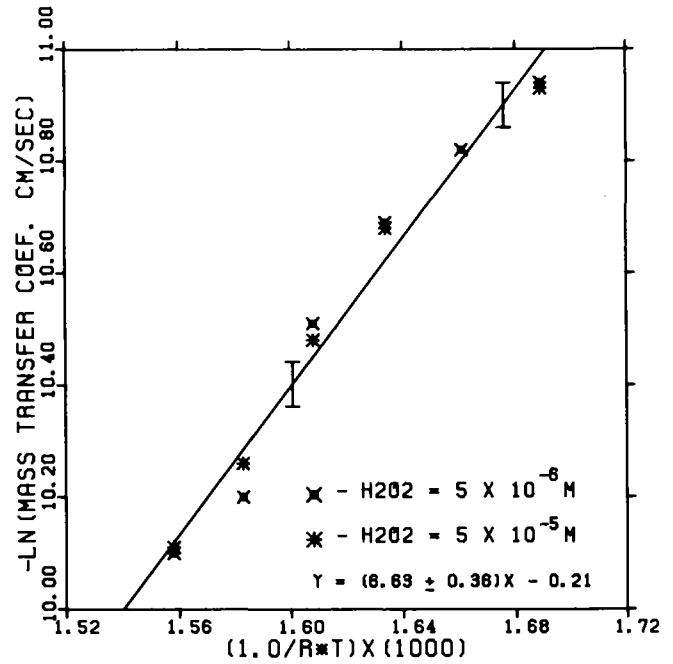


Fig. 4—Arrhenius plot showing the mass transfer coefficient for H_2O_2 , r , as a function of temperature (°K). "R" in this caption is the ideal gas constant (8.3144 J/deg/mole = 1.987 cal/deg/mole).

ratios were examined: 5, 2, 1, 0.5, and 0.25. The typical effect of total sulfate concentration on UO_2 dissolution rate is shown in Figure 5 for three ratios: 5, 1, and 0.25 (1×10^{-3} M H_2O_2). It is apparent that the presence of sulfate in concentrations of 10 to 2000 ppm causes about a 60 pct decrease in the mass transfer coefficient of H_2O_2 , regardless of the sulfate to bisulfate ratio. Addition of more sulfate up to 6000 ppm did not result in significant further decrease in the dissolution rate.

The mass transfer coefficient can be corrected for the presence of sulfate by modifying Eq. [8]:

$$r_s = (1.10 \times 10^{-5}) \exp^{-\Sigma\text{SO}_4/400} + 0.70 \times 10^{-5} \quad [9]$$

where ΣSO_4 is total sulfate and has units of ppm.

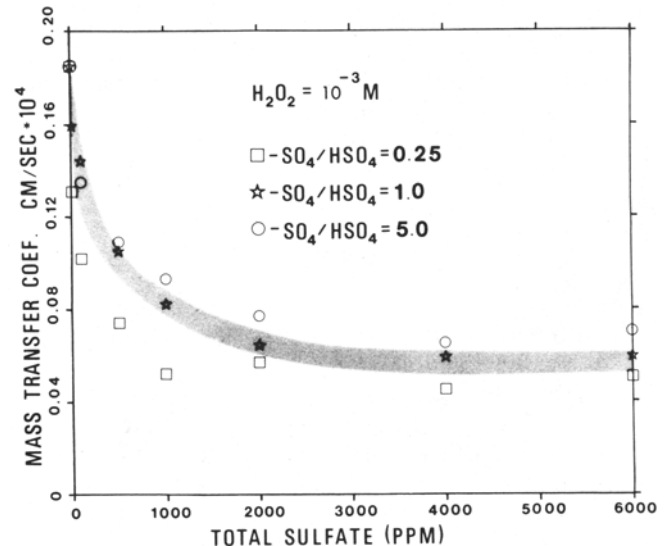


Fig. 5—Mass transfer coefficient of H_2O_2 , as a function of total sulfate concentration (ppm).

Reduction of r in the presence of sulfate, Eq. [9], can be simply related to the reaction mechanism discussed in the introduction. The proportion of sites available for oxidation, θ_1 , is influenced by the fraction of sites blocked by anion adsorption (reaction [3]). The decrease in active sites occurs rapidly with initial increase of total sulfate in solution. At sulfate concentrations above 2000 ppm the anion sites on the UO_2 surface are effectively saturated and the decrease in dissolution rate levels out (Figure 5). Evidently, θ_3 sites comprise about 60 pct of all potential θ_1 sites. The dissolution model outlined in Eqs. [4] to [7] is supported by the presence of a well-developed pattern of etching on the surface of leached UO_2 grains (Figure 6). It has been shown by Berner¹⁶ that dissolution reactions which produce etch patterns are commonly surface controlled processes. Surface controlled dissolution occurs primarily at sites of excess surface energy (dislocations, defects, etc.) which are more susceptible to attack by solutions. Greater susceptibility of some areas on a grain in comparison to other areas results in etch patterns because dislocations and defects are often oriented with respect to the crystallographic axes of a mineral (Berner¹⁶).

Close examination of many grains from our experiments indicates that initial leaching results in a polygonal set of etch grooves. With more leaching polygonally shaped pits form; the material originally outlined by the grooves has been dissolved. Small square shaped pits are commonly observed dispersed about the surface as well. This consistent etch pattern provides clear evidence that dissolution of UO_2 in H_2O_2 solutions is a surface controlled process.

The activation energy determined here, 27.2 kJ/mole, for the dissolution reaction does not provide strong evidence of a surface controlled process. An activation energy of this magnitude would normally suggest a transport controlled process (Lasaga²). But the activation energy of a dissolution reaction reflects the cumulative size of the energy barrier of all the steps involved in the reaction. Dissolution, overall, involves adsorption of H_2O_2 onto the surface, reaction at the surface, and desorption of products away from the surface. The activation energy of the combined steps can be described by:

$$E = H_{\text{ads}} + E' \quad [10]$$

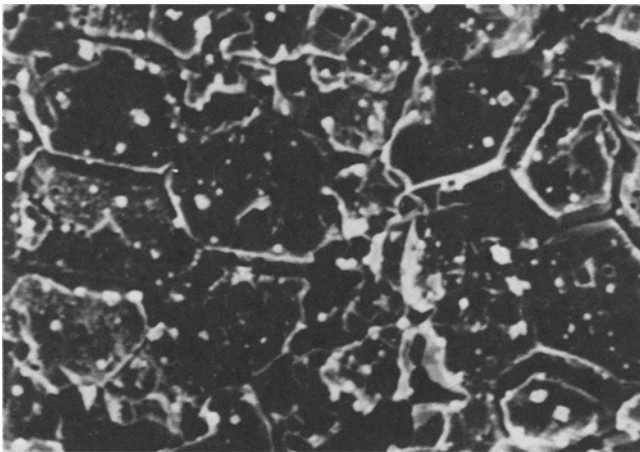


Fig. 6—Polygonal etch pattern on UO_2 surface. This UO_2 grain was leached in 1×10^{-4} M H_2O_2 at pH = 4.27. Scanning electron microscope photograph. Magnification 748 times.

where H_{ads} is the heat of adsorption of H_2O_2 onto the UO_2 surface, and E' is the activation energy of the surface reaction (Lasaga²). A large negative heat of adsorption will catalyze the reaction by reducing the overall activation energy, E , of the reaction. Data on H_{ads} of H_2O_2 onto UO_2 are not available, but such a catalyzation is reasonable. Thus, a low E value is reasonable for this surface controlled reaction and need not indicate a process controlled by the rate of aqueous transport.

B. pH Dependent Dissolution

The effect of hydrogen ion activity on dissolution rate was examined at five H_2O_2 concentrations over the range 10^{-4} to 10^{-2} M in sulfate free solutions. Above a critical pH value characteristic of the H_2O_2 concentration, initial dissolution rates show a marked decrease as the pH of the leaching solution is raised. Dissolution rates decreased with increasing pH past the critical value for all H_2O_2 concentrations examined. Figure 7 shows the results obtained for 5×10^{-4} M H_2O_2 . These results are typical. Figure 7 shows that an increase in pH produces a marked deviation from the linear kinetics at low pH (shown as the solid line in Figure 7). Experiments indicated dissolution rate continues to slow as leaching continues and that the decrease in leach rate is more pronounced and occurs at lower pH when the H_2O_2 concentration is greater.

Visual and SEM examination of the grains leached in these experiments reveal the presence of a yellow raised layer of precipitate on the UO_2 grain surface. X-ray analysis

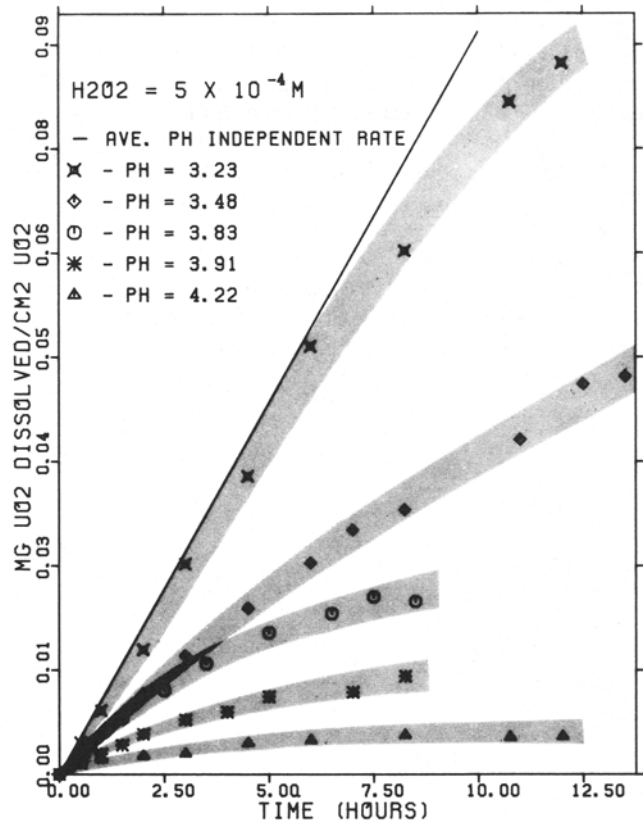


Fig. 7—Effect of pH on UO_2 dissolution. Solid line represents mean pH independent dissolution rate for 5×10^{-4} M H_2O_2 measured in solutions with pH less than 3.2.

of precipitate covered grains indicated the precipitate to be a mixture of uranium peroxide hydrates, $\text{UO}_4 \cdot \text{XH}_2\text{O}$, $X = 2$ or 4 (Debets¹⁷).

Figure 8 summarizes the pH- H_2O_2 conditions for precipitate formation. Whenever $\text{UO}_4 \cdot \text{XH}_2\text{O}$ precipitate was formed in experiments, dissolution rates were found to be decreased from the values expected for pH independent dissolution (Eq. [8]) for sulfate free solutions. Figure 8 indicates the lowest pH at which the effects of precipitation were observed. A linear relationship was determined, empirically, between pH and H_2O_2 concentration to describe the conditions of $\text{UO}_4 \cdot \text{XH}_2\text{O}$ formation and is shown by the solid line in Figure 8. Precipitate forms above the line in Figure 8, and in this pH- H_2O_2 region UO_2 dissolution rate is pH dependent. Below the line, no precipitate is formed, and the dissolution rate is pH independent and can be described by Eq. [8]. The effect of sulfate on dissolution rate for conditions of precipitate formation were not examined; a significant effect is not anticipated.

Uranium peroxide hydrate precipitation from the leaching solutions could not be predicted by an equilibrium calculation because thermodynamic data for the two and four hydrate are not available. The low effective solubility of $\text{UO}_4 \cdot \text{XH}_2\text{O}$ is well known. H_2O_2 is used to precipitate uranium from solution in hydrometallurgical processes (Brown¹⁸ and Merrit¹⁹) and in the laboratory (Watt²⁰ and Amell and Langmuir⁹). Precipitation occurs according to the following reaction (Brown¹⁸):



where "X" is equal to two or four. Reaction [11] is consistent with experimental observations in that either an increase in pH or H_2O_2 concentration favor precipitation (Figure 8).

From experimental evidence it is clear that $\text{UO}_4 \cdot \text{XH}_2\text{O}$ precipitation results in a net decrease in the rate of UO_2 dissolution due to the removal of uranium from solution. A model describing UO_2 dissolution rate in H_2O_2 solutions must at least incorporate a term to describe this precipitation of UO_2^{2+} from solution that takes place within the stability region of $\text{UO}_4 \cdot \text{XH}_2\text{O}$. The simplest model assumes the precipitate does not interfere with the leaching rate. This model (Eq. [12]) has two parts. The first term, R_d , represents the rate of dissolution of UO_2 . The second term represents the precipitation of UO_2^{2+} from solution.

$$R = R_d - (B/[\text{H}^+]^N)(C - C_{\text{sat}}) \quad [12]$$

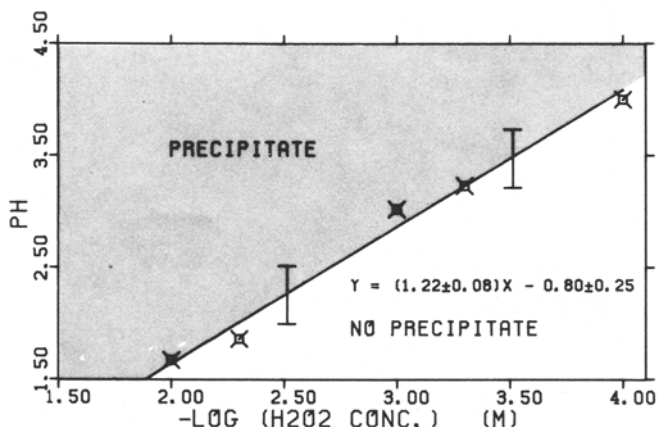


Fig. 8—Experimentally determined pH- H_2O_2 conditions of precipitate formation.

R is the net rate ($\text{mg UO}_2/\text{cm}^2$ per hour) of leaching of UO_2 ; both dissolution and precipitation are taken into account. The dissolution term is simply related to the mass transfer coefficient:

$$R_d = r[\text{H}_2\text{O}_2](\alpha)(3600)(MW_{\text{H}_2\text{O}_2}) \quad [13]$$

where r is given by Eq. [8]. The number of seconds in one hour, 3600, α , and $MW_{\text{H}_2\text{O}_2}$ convert the dissolution rate units, g/cm^2 per second to the experimental units, $\text{mg UO}_2/\text{cm}^2$ per hour.

In the precipitation term, C is the concentration (mg/liter) of UO_2^{2+} in solution, C_{sat} is the saturation concentration (mg/liter) of UO_2^{2+} with respect to $\text{UO}_4 \cdot \text{XH}_2\text{O}$ precipitation, at known H_2O_2 concentration and pH. B is a constant, $[\text{H}^+]$ is the hydrogen ion concentration (mg/liter), $[\text{H}_2\text{O}_2]$ is the H_2O_2 concentration in molarity, and N is a constant (dimensionless). Both N and B are determined from experimental data.

The precipitation term postulates, as suggested by reaction [11], that the rate of UO_2^{2+} precipitation as $\text{UO}_4 \cdot \text{XH}_2\text{O}$ is inversely proportional to H^+ concentration to the power N . Precipitation occurs only when the solution is saturated or supersaturated with respect to $\text{UO}_4 \cdot \text{XH}_2\text{O}$. When the solution is not saturated:

$$R = R_d \quad [14]$$

It can be demonstrated that Eq. [12] works well when $\text{UO}_4 \cdot \text{XH}_2\text{O}$ precipitation occurs by integrating [12] with respect to time, and comparing the calculated UO_2^{2+} concentration as a function of time to those measured in dissolution experiments. First, write R as its equivalent in terms of concentration change with time:

$$R = (dC/dt)(V_{(t)}/S) \quad [15]$$

$V_{(t)}$ is the volume (liter) of solution in the reaction vessel at time t (hours). $V_{(t)}$ is best described as a stepwise function of time. Volume is constant between sampling times but must be corrected to a new volume each time a sample is withdrawn from the kettle. S is the surface area (cm^2) of UO_2 leached in the experiment and is assumed to remain constant for the duration of an experiment. Second, for convenience, a new constant, a^* , is defined as:

$$a^* = B/[\text{H}^+]^N = \text{constant} \quad [16]$$

Equation [16] assumes pH does not change appreciably during dissolution. Experimental measurements verify this assumption. Substituting [15] and [16] into [12] and separating the variables gives Eq. [17], which can be integrated from C_{sat} to C and from t_{sat} , the time of saturation, to t :

$$\int_{C_{\text{sat}}}^C (dC)/(R_d - a^*(C - C_{\text{sat}})) = S \int_{t_{\text{sat}}}^t (dt)/V_{(t)} \quad [17]$$

Before integrating [17] an assumption will be made in regards to t_{sat} based upon experimental observations. In experiments conducted in the region of $\text{UO}_4 \cdot \text{XH}_2\text{O}$ stability it was evident that precipitation occurred very near the start of leaching. There was no observable induction period for $\text{UO}_4 \cdot \text{XH}_2\text{O}$ precipitation. Time of saturation, t_{sat} , is therefore set equal to zero and t is taken to be equal to the sampling times measured from the start of the experiment. For similar reasons C_{sat} is considered small in comparison to C and is taken to be equal to zero. Integration of [17] now gives:

$$C = (R_d/a^*)(1.0 - \exp(a^*ST_n)) \quad [18]$$

In [18], T_n is the integrated time function for the volume of leaching solution. At a particular sampling time, t_n , T_n can be expressed as:

$$T_n = \sum_0^i dt/V_{(t)} = \sum_{i=1}^n (t_i - t_{i-1})/(V_0 - (i-1)\Delta v) \quad [19]$$

where n is equal to the total number of samples of sample size Δv withdrawn from the reaction vessel. V_0 is the initial volume of solution in the reaction kettle. The sum substitutes for the initial integral because the volume is constant between sample withdrawals. We are interested only in the times at which samples are taken out and solution compositions measured.

Equation [18] predicts how the concentration, C , of UO_2^{2+} in solution should vary with time in solutions where $\text{UO}_4 \cdot \text{XH}_2\text{O}$ saturation is reached. In order to test predictions from Eq. [18], experimental data of concentrations of UO_2^{2+} measured at progressive times, were fit to an equation of the form of [18]. This was done using a Newton-Raphson method to make the best least squares fit to the dissolution data. The Newton-Raphson method adjusts values of a^* , the only unknown factor in Eq. [18], in a manner to minimize deviation between the experimental data and a curve of the form of Eq. [18]. Curves generated in this way match experimental data well overall, although the model curves do not closely match experimental points in all cases. Two comparisons of theoretical curves from Eq. [18] and measured experimental data are shown in Figures 9 and 10.

Now the value of N , the dependence of the precipitation reaction on H^+ concentration, can be determined by exam-

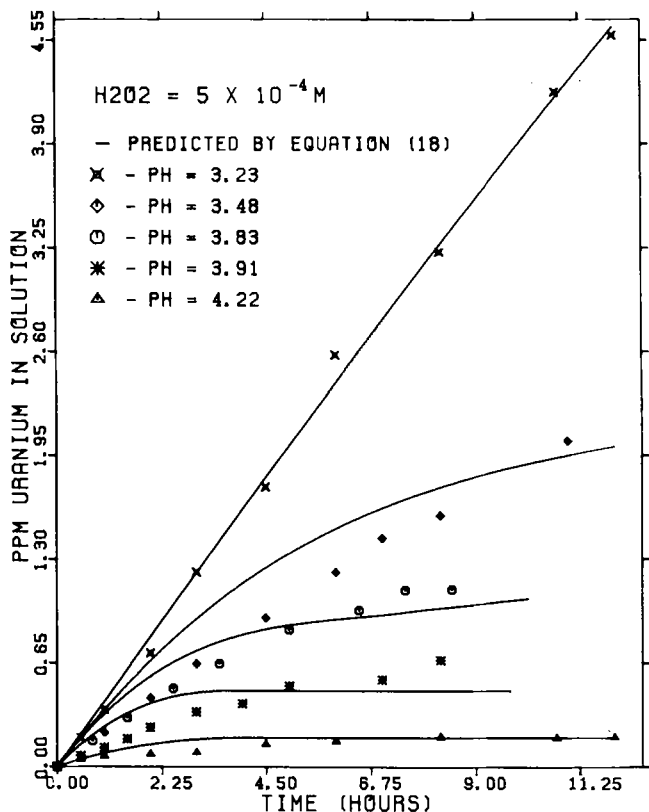


Fig. 9 — Comparison of theoretical curves and experimental data. Curves shown (solid lines) are generated from Eq. [18].

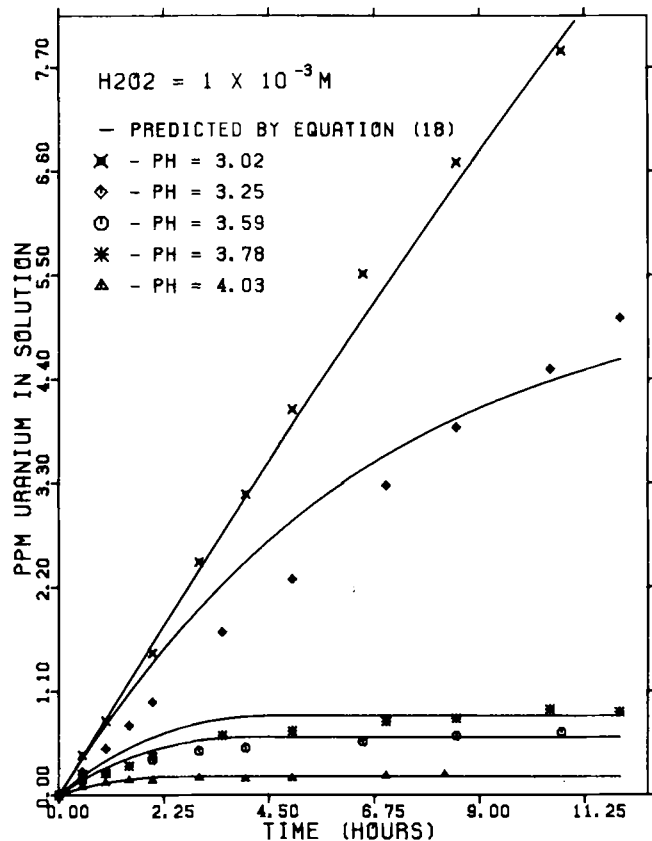


Fig. 10 — Comparison of theoretical curves and experimental data. Curves shown (solid lines) are generated from Eq. [18].

ining the dependence of a^* on H^+ concentration. Values of a^* are generated by the Newton-Raphson method of curve fitting of the dissolution rate data to Eq. [18]. N is then determined by plotting $\ln(a^*)$ vs $\ln[\text{H}^+]$ as shown in Figure 11. From Eq. [16] the relationship is given by:

$$\ln(a^*) = \ln(B) - N \ln[\text{H}^+] \quad [20]$$

A plot of $\ln(a^*)$ against $[\text{H}^+]$ will have slope $-N$ and intercept of $\ln(B)$.

In Figure 11 each line represents a least squares fit of $\ln(a^*)$ against $\ln[\text{H}^+]$ for one H_2O_2 concentration. The slopes are nearly equal for H_2O_2 concentrations of $1 \times 10^{-4} \text{ M}$ ($N = 1.87$), $5 \times 10^{-4} \text{ M}$ ($N = 1.99$), and $1 \times 10^{-3} \text{ M}$ ($N = 2.08$), lines (1), (2), and (3). The slopes are also similar for the low pH parts of the curves for $5 \times 10^{-3} \text{ M}$ ($N = 1.87$) and $1 \times 10^{-2} \text{ M}$ ($N = 2.05$), lines (4) and (5). Overall, the 5×10^{-3} and $1 \times 10^{-2} \text{ M}$ H_2O_2 data, dashed lines (6) and (7), appear to have much steeper slopes of $N = 2.96$ and $N = 2.80$, respectively. We conclude that armoring by precipitate in these cases is sufficient to slow significantly the rate of UO_2 leaching by blocking H_2O_2 from reaching the UO_2 surface, thus stopping the dissolution reaction from taking place. Armoring leads to an apparent high order dependence on pH. In these cases of complete armoring, the assumption that leaching and precipitation are independent processes cannot be considered valid, and Eq. [12] cannot be used. This breakdown of the model is not significant from a practical point of view because the rate of UO_2 dissolution is very small under conditions where armoring is complete.

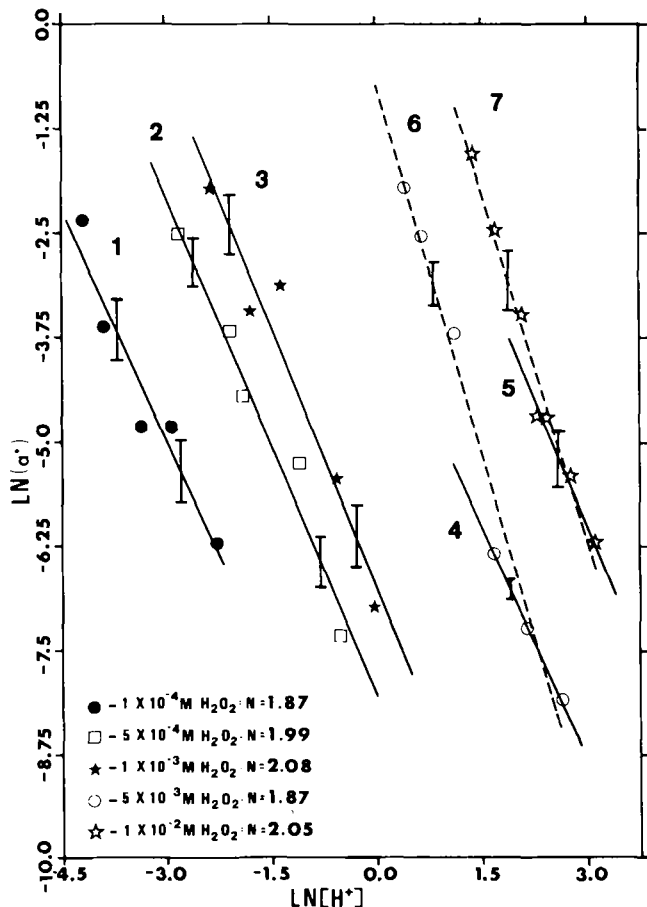


Fig. 11—Determination of constant N from a^* values generated from Eq. [18] and $\ln [H^+]$.

The slopes determined from Eq. [20] clearly indicate N is close to 2. The initial precipitation of $UO_4 \cdot XH_2O$ is inversely proportional to the square of H^+ concentration. This is consistent with the stoichiometry of reaction [11].

The rate constant B in Eq. [12] is determined from the intercept values, $\ln(B)$, from the plots of $\ln(a^*)$ against $\ln[H^+]$ from Eq. [20]. In order to determine B , the data were refit to lines with slopes taken exactly equal to -2.0 by a least squares procedure. These fitted lines yield values of B for the five H_2O_2 concentrations at which dissolution-precipitation rates were measured. The relationship is log-linear. B is given as a function of H_2O_2 concentration by:

$$B = \{(10.9 \pm 1.1) \times 10^3\} [H_2O_2]^{2.3-0.20} \quad [21]$$

A rate equation describing UO_2 dissolution for solution conditions of $UO_4 \cdot XH_2O$ precipitation, at $25^\circ C$, can now be formulated using the empirically derived expressions for the constants, N and B . The rate equation, in the form of Eq. [12] is expressed as:

$$R = R_d - \{(10.9 \pm 1.1) \times 10^3\} \times [H_2O_2]^{2.3 \pm 0.2} [UO_2^{2+}] / [H^+]^2 \quad [22]$$

where R_d is given by Eq. [13]. Equation [22] predicts how dissolution rate is affected by pH, H_2O_2 concentration, and UO_2^{2+} concentration in solutions saturated with respect to $UO_4 \cdot XH_2O$.

Since it is of interest to know the accuracy of the predicted leach rate very well, a crosscheck of Eq. [22] was made by fitting third-order polynomials to the experimental data, mg UO_2 dissolved per cm^2 at time t . This was done using a least squares method of curve fitting to a polynomial. The derivatives of the fit polynomials with respect to time give the dissolution rate at any particular time for a particular set of experimental data. This rate was checked against rates calculated by Eq. [22] for pH, H_2O_2 , and UO_2^{2+} concentrations at that time. The points in Figure 12 represent rates calculated by the polynomial time derivatives, and the solid lines are rates calculated from Eq. [22]. Figure 12 is a plot of dissolution rate for $5 \times 10^{-4} M H_2O_2$ as a function of UO_2^{2+} concentration, C , for a range of pH values. Rates calculated from the polynomial derivatives are within the error limits calculated from Eq. [22]. Figure 12 also illustrates the rapid decrease in dissolution rate which occurs as pH is raised in solutions precipitating $UO_4 \cdot XH_2O$.

The simple model proposed in Eqs. [12] and [14] that assumes precipitation does not interfere with dissolution can be further tested. If valid, the dissolution rate should increase dramatically if leach conditions are changed from pH dependent conditions that cause $UO_4 \cdot XH_2O$ precipitation to conditions in which $UO_4 \cdot XH_2O$ is not precipitated. Figure 13 shows the dissolution rate indeed immediately increases if favorable leaching conditions are restored. Because the post acidification curves do not show an offset from the preacidification curves so that they extrapolate through the origin, it is clear that acidification does not reclaim all the UO_2 that has been leached. Some leached UO_2 must remain on the uraninite grains, and this precipitate does slow the leach reaction somewhat. The model could no doubt be improved if precipitate armoring were taken into account. However, the simple model that assumes precipitate armoring does not slow the rate works remarkably well

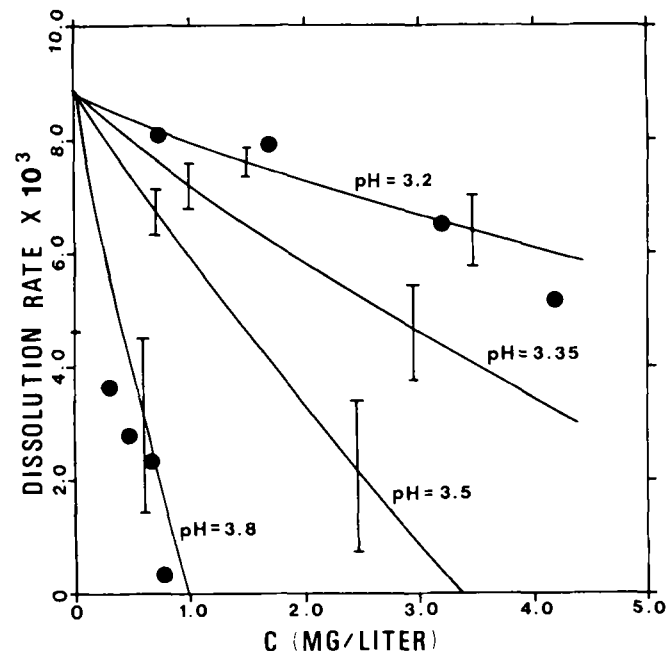


Fig. 12—Dissolution rate (mg $UO_2/cm^2/h$) as a function of C , (UO_2^{2+} concentration) for 4 pH values. Points shown are rates calculated from polynomial time derivatives from dissolution experiments with pH = 3.23 and 3.83. $H_2O_2 = 5 \times 10^{-4} M$.

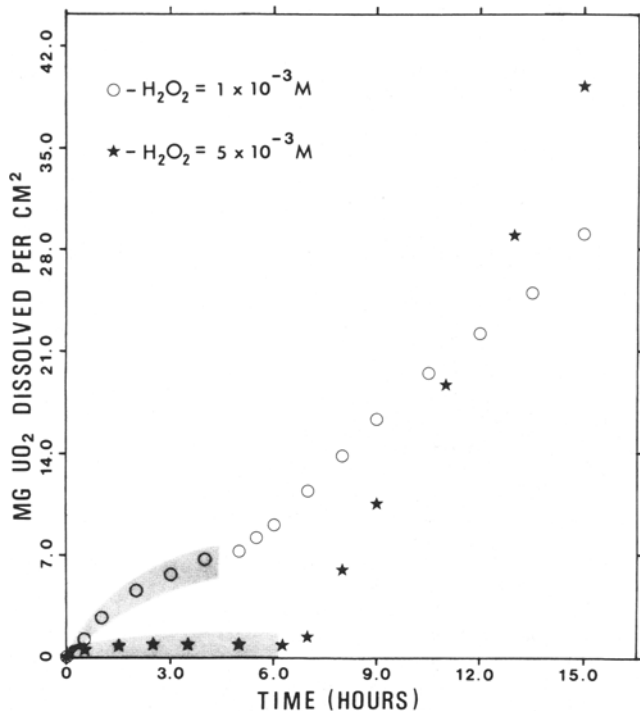


Fig. 13—Effect of acidification of leaching solution after precipitate has already formed. Shaded area indicates conditions of $\text{UO}_4 \cdot \text{XH}_2\text{O}$ formation on the UO_2 grains prior to acidification. Initial pH of the 5×10^{-3} M H_2O_2 solution was 2.16 and was acidified to 1.45 at $t = 5$ h. Initial pH of the 1×10^{-2} M H_2O_2 solution was 2.33 and was acidified to 1.43 at $t = 6.25$ h. Dissolution rate after acidification was 80 pct of predicted value (from Eq. [8]) for the 5×10^{-3} and 70 pct for 1×10^{-2} M H_2O_2 solutions.

and should usefully predict the rates of reaction for many practical applications. In our view the simplicity of the model and the fact that it requires only the present solution characteristics as input (*i.e.*, it does not require the past history of leaching which would determine the extent of armoring) are advantages that outweigh the slight loss in accuracy that results from the neglect of armoring effects.

IV. SUMMARY

The following conclusions can be made concerning the dissolution kinetics of UO_2 in acidic, H_2O_2 solutions.

- Under conditions of $\text{UO}_4 \cdot \text{XH}_2\text{O}$ undersaturation, dissolution is a first-order function of H_2O_2 concentration. Dissolution is controlled by chemical reaction rate at the UO_2 surface, and the activation energy of the dissolution reaction is 27.2 kJ/mole.
- Observations of dissolution are consistent with the following sequence of events:
 - H_2O_2 adsorbs onto the UO_2 surface and forms surface peroxide complexes.
 - Simultaneous oxidation of UO_2 and reduction of H_2O_2 occurs involving the transfer of two electrons within the surface complex. This is the slow step.
 - Reaction products then quickly dissociate from the surface.

- Addition of sulfate ions to the leaching solution caused a rate decrease probably because the preferential adsorption of the negatively charged sulfate ions onto the positively charged UO_2 surface block H_2O_2 from possible oxidation sites.
- Under conditions of oversaturation with respect to $\text{UO}_4 \cdot \text{XH}_2\text{O}$, the dissolution rate is decreased mainly due to precipitation of dissolved uranium species from solution. Precipitation is inversely proportional to the square of H^+ concentration and proportional to the degree of oversaturation.
- A rate law that assumes precipitation does not interfere with leaching works surprisingly well for conditions of $\text{UO}_4 \cdot \text{XH}_2\text{O}$ formation. The assumption that $\text{UO}_4 \cdot \text{XH}_2\text{O}$ precipitation does not armor UO_2 grains and inhibit leaching greatly simplifies the modeling of *in situ* uranium leaching. By assuming dissolution and precipitation are separate processes, the past history of leaching does not need to be known in order to model the uranium leaching process. All that needs to be known are the solution compositions and the surface area of UO_2 with which they interact at any particular time. The following equations describe UO_2 dissolution rate in terms of solution composition (pH, H_2O_2 , SO_4^{2-} , and UO_2^{2+} concentration). For conditions of $\text{UO}_4 \cdot \text{XH}_2\text{O}$ undersaturation, that is for, (from Figure 8)

$$\text{pH} < (1.22 \pm 0.08) \log[\text{H}_2\text{O}_2] - 0.8 \pm 0.25 \quad [23]$$

the rate of dissolution and H_2O_2 consumption are described by a constant mass transfer coefficient:

$$r = 1.8 \times 10^{-5} \text{ cm/sec} \quad [24]$$

Multiplication of r by the concentration of H_2O_2 in g/cm^3 gives the rate of consumption of H_2O_2 per unit surface area of uraninite in terms of g/cm^2 per second. Multiplication of the specific consumption rate of H_2O_2 by the stoichiometric ratio of UO_2 dissolved for H_2O_2 consumed (equal to the ratio of molecular weights), gives the specific leach rate of UO_2 in g/cm^2 per second.

For a system containing sulfate the mass transfer coefficient is modified:

$$r_s = (1.10 \times 10^{-5}) \exp^{-\Sigma\text{SO}_4/400} + 0.70 \times 10^{-5} \quad [25]$$

Under conditions of $\text{UO}_4 \cdot \text{XH}_2\text{O}$ formation where:

$$\text{pH} > (1.22 \pm 0.08) \log[\text{H}_2\text{O}_2] - 0.8 \pm 0.25 \quad [26]$$

H_2O_2 consumption continues to be described by [24], but the addition of UO_2^{2+} to solution is described by a mass transfer coefficient with respect to UO_2^{2+} ,

$$r_{\text{UO}_2^{2+}} = r - (1.10 \times 10^{-2})[\text{H}_2\text{O}_2]^{1.3 \pm 0.3} [\text{UO}_2^{2+}] / [\text{H}^+]^2 \quad [27]$$

In Eqs. [23] to [27]:

- r = mass transfer coefficient with respect to H_2O_2 in cm per second,
- $r_{\text{UO}_2^{2+}}$ = mass transfer coefficient with respect to UO_2^{2+} in solution in cm per second
- $[\text{H}_2\text{O}_2]$ = concentration of H_2O_2 in molarity,
- $[\text{UO}_2^{2+}]$ = concentration of UO_2^{2+} in mg/liter,
- $[\text{H}^+]$ = concentration of H^+ in mg/liter, and
- ΣSO_4 = concentration of total sulfate in mg/liter.

NOMENCLATURE

Å	angstrom (10^{-10} meters)
°C	degrees centigrade
cal	calorie
cm	centimeter
exp	exponential function
hr	hour
J	joule
kcal	kilocalorie
kJ	kilojoule
ln	natural logarithm
log	base ten logarithm
<i>M</i>	molarity
mg	milligram
ml	milliliter
mm	millimeter
$MW_{H_2O_2}$	molecular weight of H_2O_2 , 34 g/mole
MW_{UO_2}	molecular weight of UO_2 , 270 g/mole
ppb	parts per billion
ppm	parts per million
<i>r</i>	mass transfer coefficient with respect to H_2O_2 (cm per second)
$r_{UO_2^{2+}}$	mass transfer coefficient with respect to UO_2^{2+} (cm per second)
sec	second
α	stoichiometric coefficient of dissolution reaction = $(MW_{UO_2}/MW_{H_2O_2})$ (1.0 cal = 4.1840 J)

ACKNOWLEDGMENTS

The authors would like to acknowledge the support of the United States Department of Interior, Bureau of Mines, Twin Cities Research Center in this work under contract number J010065, project "Kinetic Modeling of Uranium Solution Mining". We thank particularly Dr. Robert Schmidt of the Twin Cities Research Center for his interest and encouragement. Research support was also received from the Mineral Conservation Section, College of Earth and Mineral Sciences, Pennsylvania State University. Many thanks are also extended to Dr. H. L. Barnes, Dr. A. C. Lasaga, Dr. K. Osseo-Asare, Kevin Breen, Bill

Bourcier, and Stewart Eldridge for their help, guidance, and comments on this research. The authors would also like to thank two anonymous reviewers for several very useful suggestions for improving the manuscript.

REFERENCES

1. D. R. Tweeton, G. R. Anderson, J. K. Ahlness, O. M. Peterson, and W. H. Engelman: *Soc. Min. Eng. AIME*, 1979, Preprint No. 70-43.
2. A. C. Lasaga: *Kinetics of Geochemical Processes, Reviews in Mineralogy*, A. C. Lasaga and R. J. Kirkpatrick, eds., Mineralogical Society of America, Washington, DC, 1981, vol. 8, pp. 1-67.
3. G. A. Parks: *Chem. Revs.*, 1965, vol. 65, pp. 177-98.
4. J. A. Davis, R. O. James, and J. O. Leckie: *J. Colloid Interface Sci.*, 1978, vol. 63, pp. 480-99.
5. A. J. G. Maroto: *An. Asoc. Quim. Argent.*, 1970, vol. 58, p. 187 (abs. in *Chem. Abs.*, 1971, vol. 74, 68163 pp).
6. G. A. Parks: *Equilibrium Concepts in Natural Water Systems, Advances in Chemistry Series*, Am. Chem. Soc., Washington, DC, 1967, no. 67, pp. 121-60.
7. M. J. Nicol, C. R. S. Needes, and N. P. Finkelstein: *Rep. Natn. Inst. Metall.*, PIN 171, October 1973, 37 pp.
8. C. R. S. Needes, M. J. Nicol, and N. R. Finkelstein: *Leaching and Reduction in Hydrometallurgy*, A. R. Burkin, ed., Institution of Mining and Metallurgy, London, 1975, pp. 12-19.
9. A. R. Amell and D. Langmuir: Contract No. H027219, U. S. Bureau of Mines, Dept. of the Interior, Washington, DC, 1978.
10. F. Gronvold: *J. Inorg. Nucl. Chem.*, 1955, vol. 1, pp. 357-70.
11. H. L. Barnes: *Research Techniques for High Pressure and High Temperature*, G. C. Ulmer, ed., Springer-Verlag, New York, NY, 1971, pp. 317-56.
12. A. Y. Smith and J. J. Lynch: *Field and Laboratory Methods Used by the Geological Survey of Canada*, #11, Geological Survey of Canada Paper 69-40, 1969, 9 pp.
13. G. M. Eisenberg: *Ind. Eng. Chem., Anal. Ed.*, 1943, vol. 15, pp. 327-28.
14. R. M. Smith and A. E. Martell: *Critical Stability Constants, Vol. 4: Inorganic Complexes*, Plenum Press, New York, NY, 1976, p. 82.
15. D. Langmuir: *Geoch. Cosmo. Acta*, 1978, vol. 42, pp. 547-69.
16. R. A. Berner: *Kinetics of Geochemical Processes, Reviews in Mineralogy*, A. C. Lasaga and R. J. Kirkpatrick, eds., Mineralogical Society of America, Washington, DC, 1981, vol. 8, pp. 111-34.
17. P. C. Debets: *J. Inorg. Nucl. Chem.*, 1963, vol. 25, pp. 727-31.
18. R. A. Brown: *Soc. Min. Eng. AIME*, 1980, Preprint No. 80-63.
19. R. C. Merrit: *The Extractive Metallurgy of Uranium*, Colorado School of Mines Research Institute, Golden, CO, 1971, pp. 247-48.
20. G. W. Watt, S. L. Achorn, and Marley: *J. Am. Chem. Soc.*, 1950, vol. 72, pp. 3341-43.